Predicting Vibrational Mean Free Paths in Amorphous Materials

Jason M. Larkin[1] and A. J. H. McGaughey[2,*]

[1]*Department of Mechanical Engineering*
Carnegie Mellon University
Pittsburgh, PA 15213
[2]*Department of Mechanical Engineering*
Carnegie Mellon University
Pittsburgh, PA 15213

(Dated: May 30, 2013)

Understanding thermal transport in crystalline systems requires detailed knowledge of phonons, which are the quanta of energy associated with atomic vibrations. By definition, phonons are non-localized vibrations that transport energy over distances much larger than the atomic spacing. For disordered materials (e.g., alloys, amorphous phases), with the exception of very long wavelength modes, the vibrational modes are localized and do not propagate like phonons. The Einstein model assumes that the mean free path of these localized vibrations is the average interatomic distance and that their group velocity is equal to the speed of sound. The Cahill-Pohl model assumes that the mean free path of the localized modes is equal to half of their wavelength. While these approach can be used to estimate the thermal conductivity of disordered systems, they only provide a qualitative description of the vibrations that contribute to the lattice thermal conductivity. Using lattice dynamics calculations and molecular dynamics simulations on model amorphous silicon and silica, we predict and characterize the contributions from phonons and localized vibrations to lattice thermal conductivity. The vibrational mean free paths are predicted for these two amorphous materials and the thermal conductivity accumulation function is compared with recent experimental results.

I. INTRODUCTION

The thermal conductivity of amorphous solids display unique temperature dependance compared to ordered solids.[1] Cahill argued that the lattice vibrations in a disordered crystal are essentially the same as those of an amorhous solid.[2]

Measurements by all the refs from Galli paper, including Moon.[3–9] The key to understanding such measurement is to estimate a MFP for the vibrational modes in disordered systems.

The goal of this work is to predict the MFP of vibrational modes in disordered systems. Simple Lennard-Jones systems will be studied. A perfect LJ crystal are alloyed with a species of differing mass and amorphous samples are prepared. Thermal transport will be studied to quantify and characterize the ordered and disordered contributions to lattice thermal conductivity. In particular, a more rigorous way to classify vibrational modes in disordered alloys and amorphous samples as phonon-like or diffuson will be investigated. These results will be compared to the phenomenological Einstein and Cahill-Pohl models,[? ? ?] .

The vibrational modes in these systems are characterized in the limit of propagating (phonon) and non-propagating (diffuson) modes by predicting the mode lifetimes and estimating their mean free paths. Estimating an effective dispersion relation is necessary for calculating an effective group velocity for disordered, which is crucial for transforming lifetimes to MFPs. The spectrum of phonon MFPs and the accumulated thermal conductivity are predicted for a model of amorphous silicon. Predictions of thermal conductivity using a boundary scattering model demonstrates

II. THEORETICAL FORMULATION

A. Phonons

k = sum over modes

For a perfect system, all vibrational modes are phonons.

For a perfect lattice, all vibrational modes are phonon modes, which by definition are delocalized, propagating plane waves.[?] Using the single-mode relaxation time approximation[?] to solve the Boltzmann transport equation gives an expression for thermal conductivity in direction $\mathbf{n}$,

$$k_{vib,\mathbf{n}} = \sum_{\boldsymbol{\kappa}} \sum_{\nu} c_{ph}(\boldsymbol{\kappa}_\nu)\, \boldsymbol{v}^2_{g,\mathbf{n}}(\boldsymbol{\kappa}_\nu)\, \tau(\boldsymbol{\kappa}_\nu)\,. \tag{1}$$

Here, the sum is over the phonon modes in the first Brillouin zone, $\boldsymbol{\kappa}$ is the wave vector, and ν labels the polarization branch. The phonon mode has frequency $\omega(\boldsymbol{\kappa}_\nu)$, volumetric specific heat $c_{ph}(\boldsymbol{\kappa}_\nu)$, $\mathbf{n}$-component of the group velocity vector $v_{g,\mathbf{n}}(\boldsymbol{\kappa}_\nu)$, and lifetime $\tau(\boldsymbol{\kappa}_\nu)$.

For amorphous materials, only in the low-frequency (long-wavelength) limit can the vibrational modes can be considered phonons. The amorphous materials studied in this work are isotropic, so k_{vib} and v_g are quantities indepdent of the direction $\mathbf{n}$.

The phonon mean free path (MFP),

$$\Lambda(\boldsymbol{\kappa}_\nu) = |\boldsymbol{v}_g^2(\boldsymbol{\kappa}_\nu)\,|\tau(\boldsymbol{\kappa}_\nu)\,, \tag{2}$$

is the distance the phonon travels before scattering. Because there is a spectrum of vibrational modes in cyrstalline and amorphous systems, there are typically a range of vibrational MFPs.(cite) By reducing the system feature sizes, the vibrational MFPs can be reduced due to boundary scattering.(cite)

which requires a group velocity.

Taking the phonon mode specific heat to be $c_{ph}(\boldsymbol{\kappa}_\nu) = k_B$, the phonon mode specific vibrational conductivity (Eq. (**??**)) can be written as

$$k_{vib,\mathbf{n}} = \sum_{\boldsymbol{\kappa}} \sum_{\nu} k_B D_{ph}(\boldsymbol{\kappa}_\nu)\,, \tag{3}$$

and the vibrational conductivity is determined by the phonon mode diffusitivies, defined as

$$D_{ph}(\boldsymbol{\kappa}_\nu) = v(\boldsymbol{\kappa}_\nu)^2\,\tau(\boldsymbol{\kappa}_\nu)\,. \tag{4}$$

B. Diffusons

For disordered systems, the vibrational modes are no longer pure plane-waves (i.e., phonon modes), except in the low-frequency (long-wavelength) limit. When applied in the classical limit, the Allen-Feldman (AF) theory computes the contribution of diffusive, non-propagating modes (i.e., diffusons) to thermal conductivity from[10]

$$k_{AF} = \sum_{diffusons} \frac{k_\mathrm{B}}{V} D_{AF,i}(\omega_i), \tag{5}$$

where $D_{AF,i}$ is the mode diffusivity and ω_i is the frequency of the ith diffuson. The diffusivity of diffusons can be calculated from harmonic lattice dynamics theory.[10–12]

The relative contribution of both phonons and diffusons to the total vibrational conductivity has been estimated to be approximately equal for a-Si,[13] while earlier studies find that k_{ph} is substatiantially less.[12]

C. Thermal Diffusivity Limits

k = sum c D, only for low-w, long-lambda limit does D = 1/3 v^2*tau*, *or*1/3*vLambda*

"The diffusivity D i cannot be meaningfully represented as v 2 i /3 since v i and i cannot be independently i defined. Numerically we find that D i for diffusons is of order D a/3 where a is the interparticle spacing. Also, D i is inde- pendent of the particular state i, depending only on the en- ergy as seen in Fig. 12. Our Eq. 7 for the heat conductivity is a close analog of Eq. A4.

$$\tau = \frac{2\pi}{\omega}. \tag{6}$$

$$\Lambda = \lambda. \tag{7}$$

It is not clear that these limits are equivalent if the group velocity is mode-dependent.

A high-scatter limit for the mode diffusivity is

$$D_{HS} = \frac{1}{3} v_s a, \tag{8}$$

where it is assumed that all vibrational modes travel with the sound speed, v_s, and scatter over a distance of the lattice constant, a. This diffusivity assumption leads to a high-scatter (HS) limit of thermal conductivity in the classical limit[14]

$$k_{HS} = \frac{k_\mathrm{B}}{V_b} b v_s a, \tag{9}$$

where V_b is the volume of the unit cell and b is the number of atoms in the unit cell.

It was demonstrated by Birch and Clark and then Kittel that the thermal conductivity of glasses above 20K could be interpreted using a temperature-independent diffusivity on the order of Eq. In the phonon model, this would correspond to a MFP $\Lambda = a$, too small to justify use of the model. The success of this observation implies that the dominant normal modes in most glasses are diffusons and not phonons.

While Eq and are commonly used to establish a high-scatter limit for diffusivity and thermal conductivity, predictions for a-SiGe alloys demonstrated that these are not true high-scatter limits.[11] Recently, the thermal conductivity of several materials has been measured to be significantly below the high-scatter limite Eq. .(cite)

III. CALCULATION DETAILS

A. Sample Preparation

1. *Amorphous Si*

We use models created by the Wooten-Wiener-White (WWW) algorithm as described in Ref. **?** . Sample sizes of 216, 1000, 4096, and 100,000 atoms. The Stillinger-Weber potential is then used with these samples and the denisty is set to kg/m^3, which is equivalent to a crystalline density with a lattice constant of 5.43 $\mathring{A}$. The samples were annealed

With amorphous materials, have to deal with metastability.(cite) There are many potential energy configurations (atomic positions) which are nearly equivalent in energy. At a sufficient temperature, the meta-stable states cause the equillibrium atomic positions to vary.

This can effect on the prediction of the vibrational mode lifetimes when using the normal mode decomposition method. In the time domain, the average normal mode potential and kinetic energy must be calculated and subtracted from the normal mode energy autocorrelation function. If the average energy is not specified correctly, unphysically large or small mode lifetimes can be predicted.

Anneal at 1100 K for 5 ns to remove meta-stability. The meta-stability is demonstrated by increased vs after annealing. structural relaxation: Ul =7.64X10 m/s and UT=3. 67X10, indicates that there has been structural relaxation $vs_long : 8.2715e+03, vs_tran : 3.8867e+03$

A large sample (800,000 atoms) was created from the 100,000 atom sample by treating it as a unit cell and tiling the 800,000 atom supercell. The box size is nm.

All calculations based on density of the perfect crystal with lattice constant 5.43 Ang.

2. *Amorphous SiO_2*

samples from Alan. The 24-6 LJ potential is replaced with a 12-6, which has a negligible effect on the predictions presented in this paper.

New samples of size up to 4400 atoms were created by first tiling the smaller samples, and then performing a liquid quench procedure similar to Alan. Results for these quenched, fully amorphous samples agree closely with those of the unquenched, tiled samples.

B. Simulation Details

The MD simulations were performed using LAMMPS.[15]

dt = 0.00905 , dt = 0.0005

$2^20 for 10 seeds. For the GK method, the thermal conductivity is predicted by windowed averaging the integrated heat current autoco$ SiO_2 and s-Si, a interval of the the HCACF integral can be found which is constant within the statistical noise.

The trajectories from the MD simulatoins used for the GK calcaultions (Setion) are also used in the normal mode decomposition method (Section).

The AF calculation is performed using the package GULP. A Lorentzian broadening is used of $5\delta\omega_{avg}$ and $14\delta\omega_{avg}$ for a-Si and a-SiO^2. Varying the broadening around these values does not change the resulting thermal conductivity significantly (see Section).

IV. VIBRATIONAL PROPERTIES

A. Density of States

Feldman measure the DOS using the average level spacing.[12]

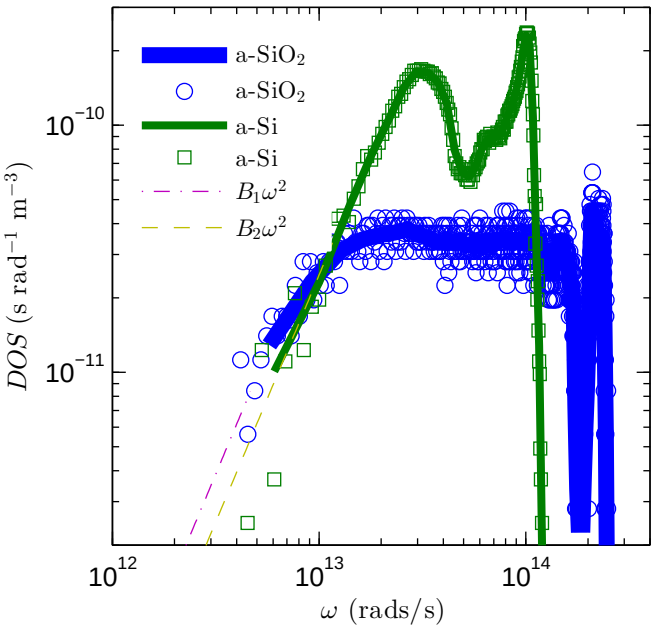

FIG. 1: film thickness dependant thermal conductivity of a-Si from experiment.

$$DOS(\omega) = \sum_i \delta\omega_i - \omega, \tag{10}$$

where a unit step function is used to broaden $\delta(\omega_i - \omega)$.
Debye Model:

$$DOS(\omega) = \frac{3 * \pi\omega^2}{2v_s^3}, \tag{11}$$

See it clearly for a-Si, only barely for a-SiO_2

estimates of the sound speeds from the elastic constants are

A fit of the DOS gives

$$v_s = \frac{1}{3}v_{s,L} + \frac{2}{3}v_{s,T}, \tag{12}$$

$$v_s = \frac{B_{mod}}{\rho}, \tag{13}$$

"The vertical lines starting on the frequency axis give the inverse participation ratios of the states, showing the quasilocalized or resonant nature of the low- est eigenstate at 4.2 meV."

"The modes of mixed character which lie outside or in between the central groups of pure plane-wave modes are typically resonances as indicated by the large values of 1/p i . How- ever, these modes are also reasonably well

interpreted as filling in the appropriate tails of Lorentzian response func- tions, modulo small statistical fluctuations to be expected in finite systems.

bigger and small Q s become less sparse, Lorentzians of fixed width will overlap increasingly, and can force out the resonant states which otherwise would inhabit the gaps. For Q of order 1/L there will always be gaps, no matter how big the system L see for instance the region near 4.1 meV in Fig. 6 where a resonance occurs, but these gaps drift toward Q 0 and 0 as L increases. Therefore the distinction between special frequencies lying in gaps, and other frequen- cies lying in Lorentzian peaks, must disappear as L increases. There are two possibilities: either resonant behavior entirely disappears, or else it remains in a diluted form and is shared uniformly by all the normal modes. That is, at any given frequency there may be isolated parts of a large sample which are particularly sensitive to oscillation at just this fre- quency and temporarily trap selected traveling waves of this frequency. If this behavior is found for all normal modes, then any one normal mode will be freely propagating almost everywhere, and it becomes a subtle matter of definition or taste whether they should be called resonances at all. ”

B. Struture Factor

Fig 4 of this work shows a dispersion extracted by locating the peaks in the structure factor.[16]

Fig. 5 discusses how since the low freq modes are sparse, there is a resonant effect between[12]

If all modes are summed over, this gives the frequency spectrum needed to construct a (nonstationary) propagating state with a pure wave vector Q and pure longitudinal or transverse polarization[11]. Locations of spectral peaks are peaked like a acoustic dispersion branches. Only low-frequency vibrations have an (approximate) wavevector in disordered systems, and there is no theorem guranteeing this.[12]

However, it is very difficult to distinguish between localized and extended modes at high frequencies on the basis of their $S(k,\nu)$ functions, as illustrated by the very similar scattering functions for a 67-meV localized and a 63-meV extended mode in Fig. 3(b).[17]

The dynamic structure factor can be useful for demonstrating the plane-wave character of low-frequency vibrations. However, on a mode-by-mode basis, it is unable in general to characterize a given mode as either localized or delocalized. Thus, it is not possible to

$$\mathbf{v}_{g,\mathbf{n}}(\tfrac{\boldsymbol{\kappa}}{\nu}) = \frac{\partial\omega(\tfrac{\boldsymbol{\kappa}}{\nu})}{\partial\boldsymbol{\kappa}}. \tag{14}$$

estimates of the sound speeds are found from using finite difference of the peaks in $S_{T,L}$ for different values of k.

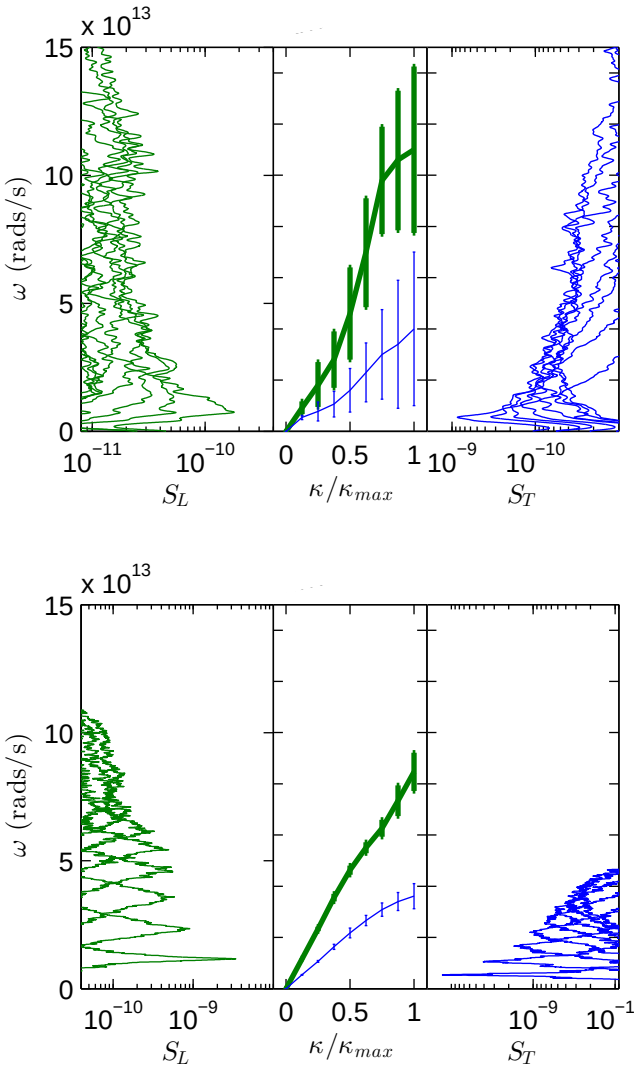

FIG. 2: film thickness dependant thermal conductivity of a-Si from experiment.

The structure factor at a VC wave vector $\boldsymbol{\kappa}_{VC}$ is defined as[18]

$$S^{L,T} = \sum_{\nu} E^{L,T}\delta[\omega-\omega], \tag{15}$$

where the summation is over the Gamma modes, E^T refers to the transverse polarization and is defined as

$$E^L = \left|\sum_b \hat{\boldsymbol{\kappa}}_{VC}\cdot e\exp\left[i\boldsymbol{\kappa}_{VC}\cdot\boldsymbol{r}_0\left(\tfrac{l=0}{b}\right)\right]\right|^2 \tag{16}$$

and E^L refers to the longitudinal polarization and is defined as

$$E^T = \left|\sum_b \hat{\boldsymbol{\kappa}}_{VC}\times e\exp\left[i\boldsymbol{\kappa}_{VC}\cdot\boldsymbol{r}_0\left(\tfrac{l=0}{b}\right)\right]\right|^2. \tag{17}$$

TABLE I: Estimated from the elastic constants, the pre-annealed group velocities are $v_{s,T,elas} = 3,670$, $v_{s,L,elas} = 7,840$ $v_{s,T,elas} = 2,541$, $v_{s,L,elas} = 4,761$

method	B_{mod} (Eq. (14))	$S_{T,L}$ (Eq. (16), (19))	DOS (Eq. (12))
a-SiO_2			
transverse	3,161	2,732	2,339
longitudinal	5,100	4,779	
a-Si			
transverse	3,886	3,699	3,615
longitudinal	8,271	8,047	

In Eqs. (17) and (18), the b summations are over the atoms in the disordered supercell, $\boldsymbol{r}_0\binom{l=0}{b}$ refers to the equilibrium atomic position of atom b in the supercell, l labels the unit cells ($l = 0$ for the supercell), α labels the Cartesian coordinates, and $\hat{\boldsymbol{\kappa}}_{VC}$ is a unit vector. Explicit disorder is included in the Gamma frequencies ω and the $3N_a$ components of the eigenvectors, e.

$$\mathbf{v}_{g,\mathbf{n}}\binom{\boldsymbol{\kappa}}{\nu} = \frac{\partial\omega\binom{\boldsymbol{\kappa}}{\nu}}{\partial\boldsymbol{\kappa}}. \tag{18}$$

A group velocity can be assigned by taking a slope of a graph of peak frequency versus wave vector. This velocity (=7X10 cm/sec) is slightly smaller than the acoustic velocity seen at smaller Q's. The mean free path is about the same as for the first peak, namely, the cell size. At larger wave vectors there is a dramatic change in the spectral shape. Insofar as they can b defined, full widths at half maximum are 30 oo f h 60eak fre quency, which corresponds to m mean free paths u p (with a generous choice of acoustic velocities) a f wi 2 or more smaller than the corresponding crystalline t th 1 wavelengths. Clearly the mod spectrum are marginally propagating, whereas the major- of energies an wave vectors, are not p opaga t'ing in any pro a e, sense. evertheless, they are extended contribute a significant heat current.[11]

Table I.

C. Mode Lifetimes

Once the group velocities are predicted using the VC dispersion, the mode lifetimes are required to predict the thermal conductivity using Eq. (**??**). As an alternative to the VC-ALD approach for predicting lifetimes, which is discussed in the next section, we first use the MD simulation-based NMD method.[19–22] In NMD, the atomic trajectories are first mapped onto the vibrational mode coordinate $q\binom{\boldsymbol{\kappa}}{\nu};t)$ and its time derivative $\dot{q}\binom{\boldsymbol{\kappa}}{\nu};t)$ by[23]

$$q\binom{\boldsymbol{\kappa}}{\nu};t) = \sum_{\alpha,b,l}^{3,n,N} \sqrt{\frac{m_b}{N}} u_\alpha\binom{l}{b};t)\, e^*\binom{\boldsymbol{\kappa}\ b}{\nu\ \alpha} \exp[i\boldsymbol{\kappa}\cdot\mathbf{r}_0\binom{l}{0}] \tag{19}$$

and

$$\dot{q}\binom{\boldsymbol{\kappa}}{\nu};t) = \sum_{\alpha,b,l}^{3,n,N} \sqrt{\frac{m_b}{N}} \dot{u}_\alpha\binom{l}{b};t)\, e^*\binom{\boldsymbol{\kappa}\ b}{\nu\ \alpha} \exp[i\boldsymbol{\kappa}\cdot\mathbf{r}_0\binom{l}{0}]. \tag{20}$$

Here, m_b is the mass of the b_{th} atom in the unit cell, u_α is the α-component of the atomic displacement from equilibrium, $\dot{u}_\alpha$ is the α-component of the atomic velocity, and t is time. The total energy of each vibrational mode, $E\binom{\boldsymbol{\kappa}}{\nu};t)$, is calculated from

$$E\binom{\boldsymbol{\kappa}}{\nu};t) = \frac{\omega\binom{\boldsymbol{\kappa}}{\nu}^2}{2} q\binom{\boldsymbol{\kappa}}{\nu};t)^*\, q\binom{\boldsymbol{\kappa}}{\nu};t) + \frac{1}{2}\dot{q}\binom{\boldsymbol{\kappa}}{\nu};t)^*\, \dot{q}\binom{\boldsymbol{\kappa}}{\nu};t)\,. \tag{21}$$

The vibrational mode lifetime is predicted using

$$\tau\binom{\boldsymbol{\kappa}}{\nu} = \int_0^{t^*} \frac{< E\binom{\boldsymbol{\kappa}}{\nu};t)\, E >}{< EE >} dt, \tag{22}$$

Lifetimes in amorphous silicon predicted before using a normal mode approach, but mode-by-mode properties were not presented.[24]

Lifetimes were predicted using anharmonic lattice dynamics, but no thermal transport properties were predicted.[25]

Thermal diffusivity was predicted for a percolation network which showed Rayleigh type scattering dependance in the low-frequency limit.[26]

Thermal diffusivity has been predicted using a wave-packet method

The lifetimes of vibrational modes in a-Si were predicted using normal mode decomposition.[13]

"To implement Eq. 6 one must know the correct Q dependence of Q . As shown in Fig. 8, the fitted values scatter too much to guide the extrapolation well. In principle, at very small Q one should get a form Q CQ 4 which corresponds to Rayleigh scattering of sound waves from the structural disorder. The data of Fig. 8 do not fit a Q 4 law; the Q 2 curve shown in the figure is a better fit. Two experiments13,15 but not a third35 and one calculation18 on a-SiO2 have also given Q 2 . We do not know a theory which can give this law in a harmonic model.

"The conclusion is that intrinsic harmonic glassy disorder contained in our finite calculation kills off the heat-carrying ability of propagons rapidly enough without invoking any exotic mechanism. Our (T) curve is reminiscent of the ex- periments of Zaitlin and Anderson after holes are introduced to enhance the elastic damping of long-wavelength modes. The plateau disappears from their data in much the same way that it disappears from our theory due to extra damping of small-Q propagons.

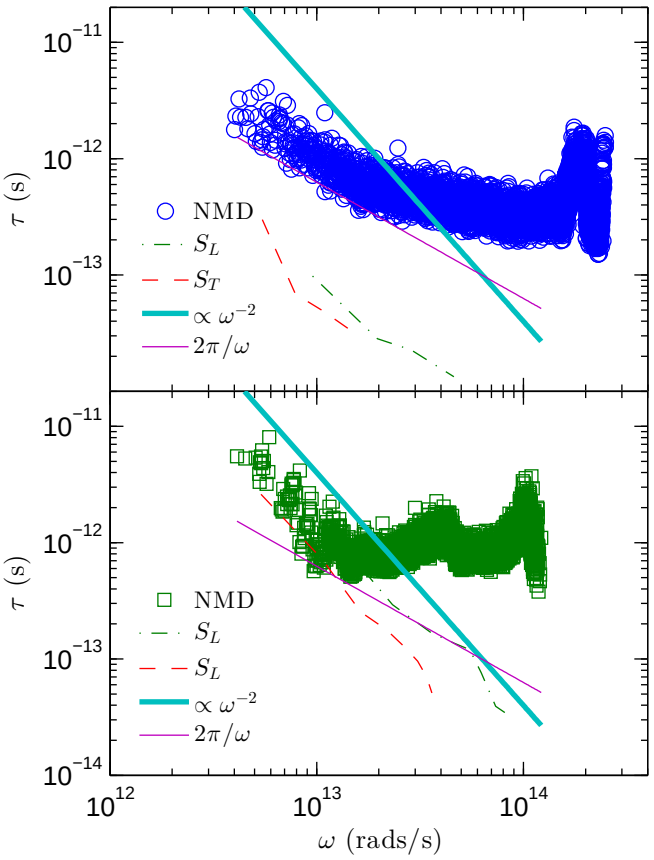

FIG. 3: film thickness dependant thermal conductivity of a-Si from experiment.

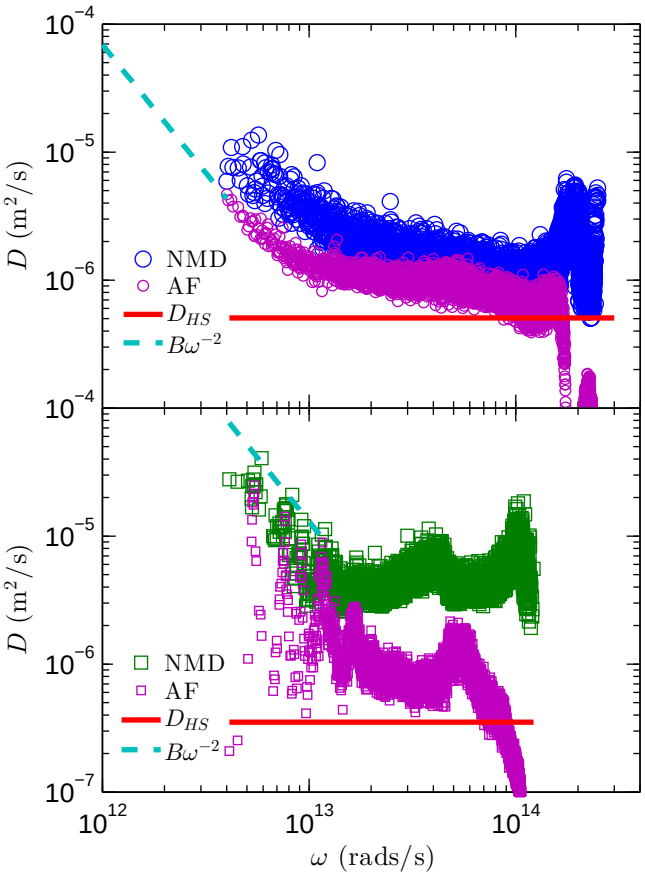

FIG. 4: film thickness dependant thermal conductivity of a-Si from experiment.

D. Diffusivities

E. Mean Free Paths

V. THERMAL CONDUCTIVITY

A. Bulk

Assuming the thermal conductivity form Eq. for the lowest frequency modes in the system, the thermal conductivity as a function of the system size takes the form

$$\frac{k(N_0)}{k_{bulk}} = 1 - \frac{c_0}{N_0}, \tag{23}$$

"We find that we cannot define a wave vector for the majority of the states, but the intrinsic harmonic diffusivity is still well-defined and has a numerical value similar to what one gets by using the Boltzmann result, replacing v by a sound velocity and replacing l by an interatomic distance a. "[11]

"In order to fit the experimental sc(T) it is necessary to add a Debye- like continuation from 10 meV down to 0 meV. The harmonic diffusivity becomes a Rayleigh m law and gives a divergent (T) as T O. To eliminate this we make the standard assumption of resonant- plus-relaxational absorption from two-level systems (this is an anharmonic effect which would lie outside our model even if it did contain two-level systems implicitly). "[11]

$$k = \int_0^{\omega_{cut}} \frac{d\omega DOS(\omega)C(\omega)D(\omega)}{V} + \frac{1}{V}\sum_i C(\omega)D(\omega) \tag{24}$$

Debye model. $k_tot = k_phonon + k_AF. For lack of a rigorous definition of phonon vs diffusion, we will d$ k_debye.

B. Accumulation

C. Discussion

VI. SUMMARY

Table I.

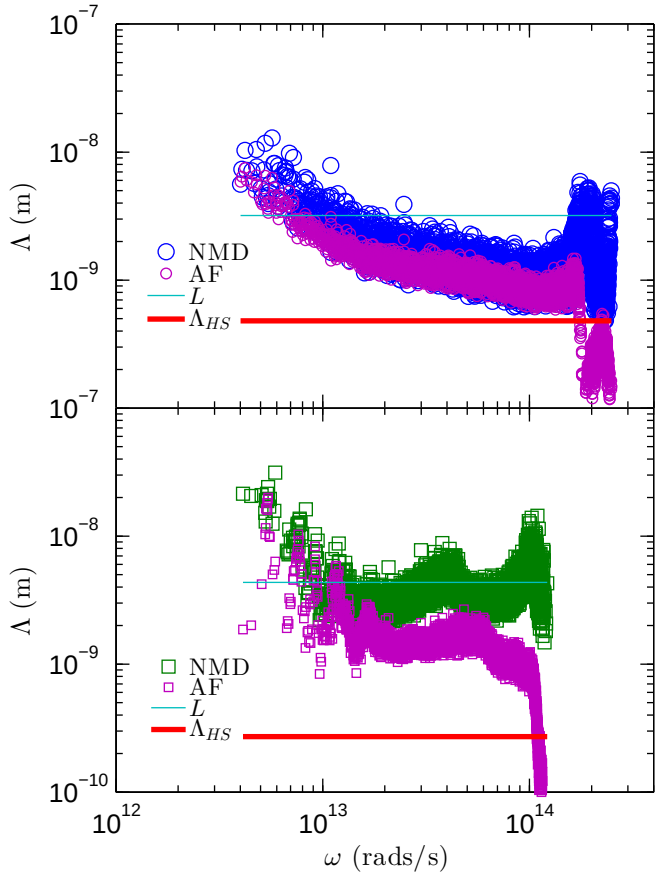

FIG. 5: film thickness dependant thermal conductivity of a-Si from experiment.

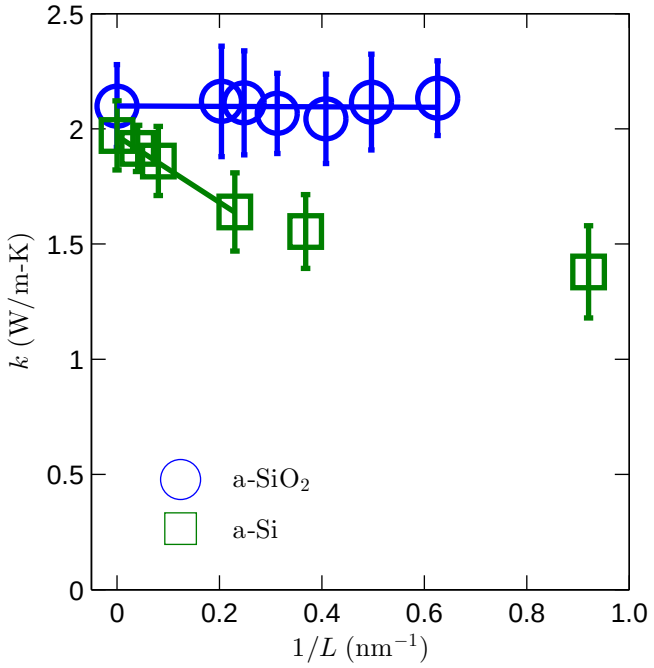

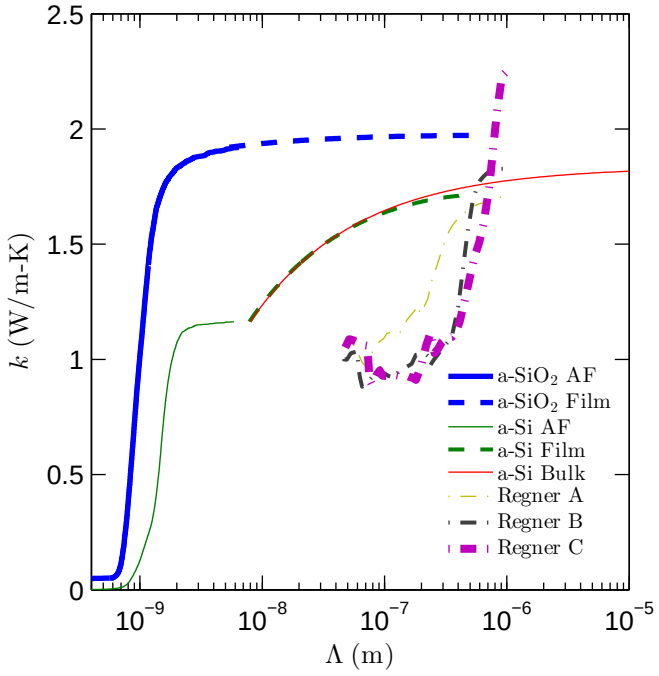

FIG. 7: film thickness dependant thermal conductivity of a-Si from experiment.

* Electronic address: mcgaughey@cmu.edu

[1] J. J. Freeman and A. C. Anderson, Physical Review B **34**, 5684\textbackslash965690 (1986).

[2] D. G. Cahill, S. K. Watson, and R. O. Pohl, Phys. Rev. B **46**, 61316140 (1992), URL http://link.aps.org/doi/10.1103/PhysRevB.46.6131.

[3] H. Wada and T. Kamijoh, Japanese Journal of Applied Physics **35**, L648L650 (1996), URL http://jjap.jsap.jp/link?JJAP/35/L648/.

[4] B. L. Zink, R. Pietri, and F. Hellman, Physical Review Letters **96**, 055902 (2006), URL http://link.aps.org/doi/10.1103/PhysRevLett.96.055902.

[5] H.-S. Yang, D. G. Cahill, X. Liu, J. L. Feldman, R. S. Crandall, B. A. Sperling, and J. R. Abelson, Phys. Rev. B **81**, 104203 (2010), URL http://link.aps.org/doi/10.1103/PhysRevB.81.104203.

[6] D. G. Cahill, M. Katiyar, and J. R. Abelson, Physical Review B **50**, 60776081 (1994).

[7] B. S. W. Kuo, J. C. M. Li, and A. W. Schmid, Applied Physics A: Materials Science & Processing **55**, 289296 (1992), ISSN 0947-8396, 10.1007/BF00348399, URL http://dx.doi.org/10.1007/BF00348399.

[8] S. Moon, International Journal of Heat and Mass Transfer **45**, 24392447 (2002), URL http://linkinghub.elsevier.com/retrieve/pii/S0017931001008477.

[9] X. Liu, J. L. Feldman, D. G. Cahill, R. S. Crandall, N. Bernstein, D. M. Photiadis, M. J. Mehl, and D. A. Papaconstantopoulos, Phys. Rev. Lett. **102**, 035901 (2009), URL http://link.aps.org/doi/10.1103/PhysRevLett.102.035901.

[10] P. B. Allen and J. L. Feldman, Physical Review B **48**, 1258112588 (1993).

[11] J. L. Feldman, M. D. Kluge, P. B. Allen, and F. Wooten, Physical Review B **48**, 1258912602 (1993).

[12] J. L. Feldman, P. B. Allen, and S. R. Bickham, Phys. Rev. B **59**, 35513559 (1999), URL http://link.aps.org/doi/10.1103/PhysRevB.59.3551.

[13] Y. He, D. Donadio, and G. Galli, Applied Physics Letters **98**, 144101 (2011).

[14] D. Cahill and R. Pohl, Annual Review of Physical Chemistry **39**, 93121 (1988).

[15] S. Plimpton, Journal of Computational Physics **117**, 1 19 (1995), ISSN 0021-9991, URL http://www.sciencedirect.com/science/article/pii/S0021999185

[16] V. Vitelli, N. Xu, M. Wyart, A. J. Liu, and S. R. Nagel, Phys. Rev. E **81**, 021301 (2010), URL http://link.aps.org/doi/10.1103/PhysRevE.81.021301.

[17] R. Biswas, A. M. Bouchard, W. A. Kamitakahara, G. S. Grest, and C. M. Soukoulis, Phys. Rev. Lett. **60**, 22802283 (1988), URL http://link.aps.org/doi/10.1103/PhysRevLett.60.2280.

[18] P. B. Allen, J. L. Feldman, J. Fabian, and F. Wooten, Philosophical Magazine B **79**, 17151731 (1999).

[19] A. J. C. Ladd, B. Moran, and W. G. Hoover, Physical Review B **34**, 50585064 (1986).

[20] A. J. H. McGaughey and M. Kaviany, Physical Review B **69**, 094303 (2004).

[21] J. E. Turney, PhD thesis, Carnegie Mellon University, Pittsburgh, PA (2009).

[22] J. M. Larkin, J. E. Turney, A. D. Massicotte, C. H. Amon, and A. J. H. McGaughey, to appear in Journal of Computational and Theoretical Nanoscience (2012).

[23] M. T. Dove, *Introduction to Lattice Dynamics* (Cambridge, Cambridge, 1993).

[24] S. R. Bickham and J. L. Feldman, Phys. Rev. B **57**, 1223412238 (1998), URL http://link.aps.org/doi/10.1103/PhysRevB.57.12234.

[25] J. Fabian and P. B. Allen, Phys. Rev. Lett. **77**, 38393842 (1996), URL http://link.aps.org/doi/10.1103/PhysRevLett.77.3839.

[26] P. Sheng and M. Zhou, Science **253**, 539542 (1991), URL http://www.sciencemag.org/content/253/5019/539.abstract.